

## Degradation of photovoltaic backsheets: Comparison of the aging induced changes on module and component level

Marlene Knausz,<sup>1</sup> Gernot Oreski,<sup>1</sup> Gabriele C. Eder,<sup>2</sup> Yuliya Voronko,<sup>2,3</sup> Bernadette Duscher,<sup>3</sup> Thomas Koch,<sup>3</sup> Gerald Pinter,<sup>4</sup> Karl A. Berger<sup>5</sup>

<sup>1</sup>Polymer Competence Center Leoben GmbH, 8700 Leoben, Austria

<sup>2</sup>OFI Austrian Research Institute for Chemistry and Technology, 1030 Vienna, Austria

<sup>3</sup>Institute of Materials Science and Technology, Vienna University of Technology, 1060 Vienna, Austria

<sup>4</sup>Institute of Materials Science and Testing of Plastics, University of Leoben, 8700 Leoben, Austria

<sup>5</sup>AIT Austrian Institute of Technology, 1210 Vienna, Austria

Correspondence to: M. Knausz (e-mail: marlene.knausz@pccl.at)

**ABSTRACT:** In reliability testing of components for PV modules an always remaining question is about material (in)compatibilities and synergistic effects and thus, how results of singly tested materials correlate with materials aged within PV modules. Testing of single materials would simplify sample preparation, reduce costs and offer more testing options. Therefore the main objective of this study was to compare the aging behavior of single backsheets with that of backsheets incorporated within PV modules. Four different types of backsheets were chosen, all of them comprising of polyethylene terephthalate (PET) core layers, but differing outer protection layers. Test modules using identical components, varying only in the type of backsheet used were produced and damp heat aged (85°C/85% RH  $\leq$  2000 h). The results revealed no influence of the PV module lamination on the thermal characteristics of the polymeric backsheets. Even after DH aging, differences between single and module laminated backsheets were negligible. Degradation effects of PET could be detected for all aged sheets by thermal analysis and were confirmed by tensile tests and rheological measurements. Thus, it can be stated that testing of single PET based backsheets under DH aging conditions is a practicable way to investigate the applicability of a new backsheet. © 2015 Wiley Periodicals, Inc. *J. Appl. Polym. Sci.* **2015**, *132*, 42093.

**KEYWORDS:** ageing; degradation; differential scanning calorimetry (DSC); mechanical properties; thermal properties

Received 28 October 2014; accepted 10 February 2015

DOI: 10.1002/app.42093

### INTRODUCTION

In PV industry, discussions about reliability testing of materials/modules are still holding on. Of special interest is the question, whether the individual components/materials should be tested as single materials or laminated within a PV module. On the one hand component testing would simplify sample preparation, lower the costs, and offer more testing options for the materials as they are often destructive. On the other hand there remains always the important question of material (in)compatibility and synergistic effects and thus, how results of tested single aged materials correlate with materials aged within PV modules. Interestingly no literature could be found which deals with this question.

In case of solar cell encapsulants, testing of whole modules is preferred as some interactions (e.g. PID, snail tracks, corrosion, yellowing...) can not be reproduced by aging of the single materials. Merely a principal applicability, preselection or

process improvements can be achieved by testing of encapsulants as single materials.

Accelerated aging and testing of backsheet films, instead, seem to be less critical with respect to the installation situation as fewer failure/degradation cases occur in combination with other PV module components. Reported failures of backsheets are delamination within the multilayer laminate, embrittlement leading to cracks, yellowing etc.<sup>1–3</sup> Yellowing of backsheets, however, is reported to have no influence on the electrical performance of the modules.<sup>1</sup> The worst failures within backsheets are cracks and delaminations as they allow enhanced water vapor and oxygen ingress into the PV module and can cause safety problems due to the loss in isolation properties. Water vapor is known to have a critical impact on various degradation phenomena like corrosion of metal-, cell parts, potential induced degradation (PID) of PV modules and encapsulant decomposition.<sup>4,5</sup> Therefore, these failure modes can reduce the performance of a PV module and shorten its lifetime.

**Table I.** List of Backsheets Used

Abbreviation	Inner layer	Core layer	Outer layer	Thickness ( $\mu\text{m}$ )
B1	PVF (37)	PET (250)	PVF (37)	340
B2	PVDF (19)	PET (250)	PVDF (19)	305
B3	EVA/PE (1.25)	PET (190); aluminum (12)	PET (50)	390
B4	EVA/PE (1.25)	PET (190)	PET (50)	375

Thicknesses of individual layers are listed in parentheses ( $\mu\text{m}$ ).

To fulfill all requirements most backsheet films for PV modules are multilayer composites comprising of three or more polymer layers. The outer layers have to be resistant against various weathering impact factors (e.g. irradiance, humidity, . . .). Often used protection layers are fluoropolymers e.g. polyvinylfluoride (PVF), polyamide (PA), or polyethylene terephthalate (PET). In most cases, the backsheets exhibit a symmetrical construction with identical polymers used for the inner and the outer protection layer varying only in the amount and type of stabilizers added. The inner layers are often additionally equipped with an adhesion layer or functionalized surface allowing optimized adhesion to the encapsulant material. The main purpose of the core layer is to provide mechanical stability, barrier against water vapor and oxygen and electrical isolation. The most frequently used polymer for this purpose is PET. In some cases also barrier layers, e.g., aluminum or silicon oxide ( $\text{SiO}_x$ ) are additionally incorporated between protection and core layer in order to improve the barrier properties of the backsheet.<sup>6</sup>

Previous studies have shown that hydrolysis is the dominant aging mechanism of PET under DH conditions, whereas the other materials used in the backsheets like e.g., fluoropolymers or polyamides are not affected significantly by exposure to high humidity at elevated temperatures.<sup>6-9</sup> Therefore, this article focuses on the description of the aging behavior of the PET core layers of various polymeric multilayer backsheets as under these conditions the stability of this layer defines the reliability of the whole backsheet. Hydrolysis of PET results in chain scission (=polymer degradation) leading to embrittlement, but also to physical aging processes like postcrystallization. Both may lead to a loss in the mechanical stability like e.g., crack formation in the inner PET layer of the backsheets and can be detected very well with tensile testing.<sup>9-11</sup>

Hence, the main aim of this article is to investigate and compare the aging behavior, i.e. the stage of hydrolytic degradation of PV backsheets with PET core layers, which were exposed to damp heat conditions as single films and laminated within PV modules. The stage of hydrolytic degradation/chain scission will be determined by differential scanning calorimetry (module and single aged films) and tensile tests (single aged films). In order to support the results, additional rheological measurements were carried out to verify the assumption of polymer chain degradation (decrease of average molecular mass) upon aging. The influence of material interactions on the reliability of the PET core layer within the PV module will be discussed.

## MATERIALS AND METHODS

In this study the aging behavior of four different types of backsheets from three different producers was investigated, all of

them containing PET core layers. The outer/inner layers of the backsheets were (i) fluoropolymers (symmetric composition) or (ii) stabilized PET on the outer side and ethylene vinylacetate (EVA)/polyethylene (PE) as primer on the inner side. Test modules comprising of a glass front sheet (float glass, 2 mm), fast cure EVA as encapsulant (Vistasolar 486.00, SolutiaSolar GmbH, 455  $\mu\text{m}$ ), 6 polycrystalline Si-cells and polymeric backsheets were fabricated in a standard lamination process. The composition of all test modules was identical except for the type of backsheet used, a description of the backsheet films investigated within this study is given in Table I. Single backsheet films and one set of test modules were exposed to damp heat (DH) conditions at 85°C and 85% relative humidity (RH) for 1000 and 2000 h. A second set of test modules and backsheets were kept as original reference samples.

The thermal behavior was characterized with differential scanning calorimetry (DSC) using a Perkin Elmer DSC 4000. Measuring program and parameters are listed in Table II. Samples of the backsheets ( $\sim 10$  mg) were cut and put in 50  $\mu\text{L}$  pans with perforated lids. Samples of module sheets were taken from the edge areas of the modules. For every evaluation, an average of at least two sample runs was taken. Melting points, melting enthalpies and crystallization temperatures were evaluated according to ISO 11357-3.<sup>12</sup>

Tensile tests were carried out on a Zwick Z001 according to EN ISO 527-3,<sup>13</sup> the test specimen were cut before accelerated aging according to specimen type 2 (150 mm x 15 mm). The test speed used was 50 mm/min. From a total of at least five specimens for each test series, the average values for yield stress ( $\sigma_Y$ ), yield strain ( $\epsilon_Y$ ), stress at break ( $\sigma_B$ ), and strain at break ( $\epsilon_B$ ) were deduced.

As a good verification of changes in molecular mass, melt rheological measurements were carried out on an Anton Paar MCR

**Table II.** Experimental Parameters for DSC Measurements (nitrogen atmosphere)

	Start	End	time/ramp
Isotherm segment	20°C		5 min
1. Segment	20°C	270°C	10°C/min
Isotherm segment	270°C		5 min
2. Segment	270°C	20°C	10°C/min
Isotherm segment	20°C		5 min
3. Segment	20°C	270°C	10°C/min

301 device in oscillatory mode. A parallel plate geometry (diameter 25 mm) was used. As the PET core layer is the dominating material in the backsheet and to eliminate overlaying effects the outer and inner layers and the adhesives were removed. To achieve a gap width, i.e. sample height, of 0.6 mm the dried films were carefully stacked to ensure a bubble free melt. Oscillation amplitude  $\gamma$  was 6% and the angular frequency  $\omega$  was 1 rad/s. The measurements were done at 270°C under nitrogen atmosphere.

## RESULTS AND DISCUSSION

In the following the results will be described and discussed considering at first the differences in the DSC curves between single backsheets and sheets incorporated into modules in the original state. Then the aging (DH storage) induced changes on module and component level will be compared. These results obtained from the thermal analysis of the polymeric sheets will then be compared to results from tensile tests (only from the single backsheets) and the rheological measurements on the PET core layers. The description of the results is focused on the aging behavior of the PET core layer, which is mainly responsible for the mechanical stability.<sup>7,8</sup>

### DSC Results

**Initial State.** Processes like melting of crystallites formed during postcrystallization or tempering are irreversible as their impact on the DSC curve can be seen only in the first but not in the second heating run. Glass transitions or the thermodynamic melting of a polymer are reversible effects and will, thus, be seen in each heating run irrespective of the history of the polymer. Therefore in the first heating curve of a DSC measurement all reversible and irreversible effects are determined including the information on the thermal and mechanical history of a polymer like physical changes (postcrystallization, changes in the crystal structure...) having taken place in the material upon processing or aging.<sup>14</sup> It reflects the so called “current state of a polymer” and is the commonly used curve for the evaluation of the application relevant behavior of a material. The second heating run gives information on material specific constants and includes only reversible effects. It plays a subordinate role for the analysis of aging induced changes.

The information obtainable from the crystallization behavior (=cooling run) is rarely discussed in standard literature. However, it bears evidence about changes in the chemical structure of a material like e.g. the decrease of molecular mass due to polymer chain scission etc.<sup>14,15</sup> As this work focuses on the aging behavior of PET which means postcrystallization (physical aging) and hydrolysis (chemical aging) both, 1.heating and cooling curves were evaluated and are presented in this article.

Postcrystallization of polymers results in an increase in the melting enthalpy as well as a shift to higher melting temperatures. Hydrolysis induces polymer chain scission which goes along with a decrease in the molecular mass and leads to a shift of the crystallization temperature to higher values as well as to an increase in the crystallization enthalpy.<sup>14</sup>

Exemplarily the DSC runs (1. heating, cooling, 2. heating) of the backsheet B1 (single and module laminated sheet of the ini-

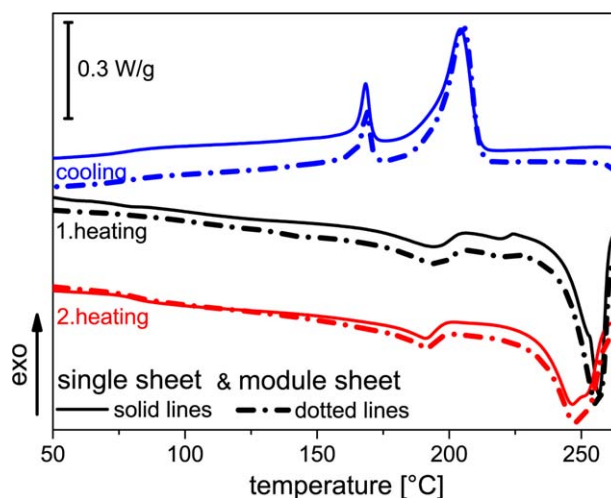


**Figure 1.** DSC curves of the initial state of single (line) and module laminated backsheet (dotted line) of B1. [Color figure can be viewed in the online issue, which is available at [wileyonlinelibrary.com](http://wileyonlinelibrary.com).]

tial state) are shown in Figure 1. In the 1.heating curve, the first melting peak can be attributed to the PVF outer layer ( $T_m = 194^\circ\text{C}$ ). The highest melting peak with respect to temperature and area is attributed to the melting of the main fraction of the PET crystallites ( $T_m = 256^\circ\text{C}$ ).

A secondary melting peak of the PET core layer was found at  $219^\circ\text{C}$ . This secondary melting peak can be attributed to small crystallites, which are formed during exposure at elevated temperatures. This peak was not detected in the second heating run which confirms its irreversible, aging induced character. The first crystallization peak in the cooling curve is attributed to PET ( $T_c = 205^\circ\text{C}$ ) and the second to PVF ( $T_c = 169^\circ\text{C}$ ). At the second heating run the PVF melting peak was detected at  $192^\circ\text{C}$  and the PET melting peak at  $248^\circ\text{C}$ .

In general, all backsheets showed comparable DSC curves for samples taken from single sheets to those taken from modules (exemplarily see Figure 1). This confirms that the lamination process of the PV module, although enhanced temperatures (up to  $150^\circ\text{C}$ ) are involved, have no influence on the thermal properties of the backsheets. Assumedly the lamination times of maximum 30 min do not lead to physical changes in the PET core layer. As expected there were also no glass transitions and/or cold-crystallization peaks observable for PET. This is an indication for a high crystalline material.<sup>14</sup> PET used for PV module backsheets has to be hydrolysis resistant, which can be achieved by enhancing the crystallinity of the material by heat treatment as well by the addition of stabilizers.

The detected temperature maxima of the peaks in the heating/cooling curves of the fluoropolymer outer layers (B1 and B2, see Figure 2), EVA/PE inner layers of B3 and B4 (see Figure 3) are compiled in Table III. The melting peaks observed at  $110^\circ\text{C}$  and  $127^\circ\text{C}$  of samples B3 and B4 are attributed to the melting of the inner layers (see Figure 3). Crosslinked EVA commonly used as encapsulant for PV modules has a vinylacetate (VA) content of  $\sim 30\%$  (w/w) and melts in the temperature region between  $30$  and  $70^\circ\text{C}$ .<sup>16</sup> Therefore the first melting peak at

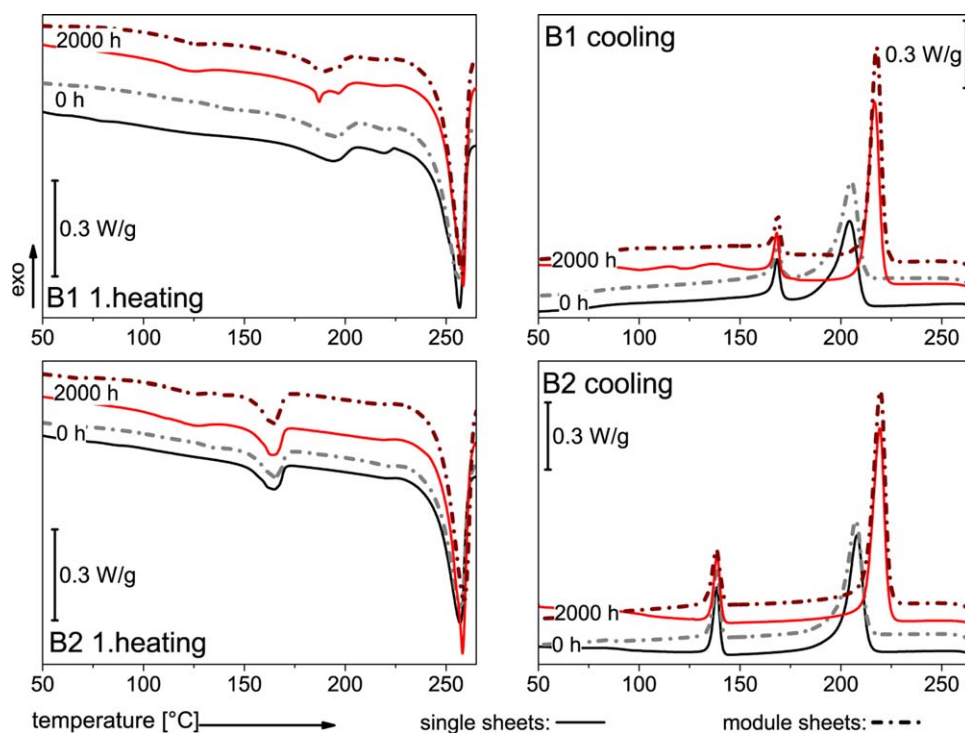


**Figure 2.** DSC heating and cooling curve of B1 (top) and B2 (bottom) for the initial state and aged (2000 h DH) samples. [Color figure can be viewed in the online issue, which is available at [wileyonlinelibrary.com](http://wileyonlinelibrary.com).]

110°C indicates that the ethylene-vinylacetate has a very low VA content and mainly consists of longer chain segments of ethylene (melting region PE  $\sim$ 130–145°C). The second melting peak

at 127°C can be attributed to an additional PE layer in the backsheet. Both assumptions were confirmed by additional ATR imaging measurements.

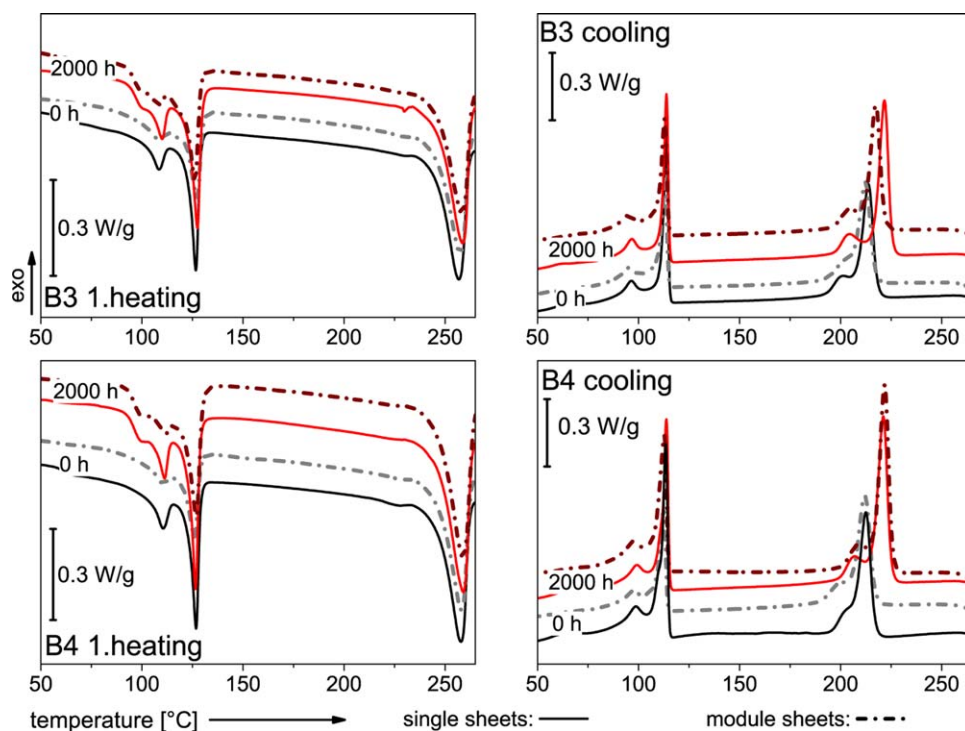


**Figure 3.** DSC heating and cooling curves of B3 (top) and B4 (bottom) for the initial state and aged (2000 h DH) samples. [Color figure can be viewed in the online issue, which is available at [wileyonlinelibrary.com](http://wileyonlinelibrary.com).]



**Table III.** Detected Peaks from the DSC Heating/Cooling Curve of the Outer and/or Inner Layers of the Single Backsheets in the Initial State

Backsheet		Heating				Cooling			
		Melting peak (°C)				Cooling peak (°C)			
Abbr.	Layer	Single sheet		Module sheet		Single sheet		Module sheet	
B1	PVF	194		195		168		169	
B2	PVDF	165		165		139		139	
B3	EVA/ PE	109	128	109	127	96	114	95	113
B4	EVA/ PE	111	127	111	126	99	113	98	112

The melting region of PET for all backsheets was found to be rather broad (230–270°C) but the maximum of the peak was constant in a very narrow temperature range between 256 and 258°C (standard deviation of each materials melting point smaller than 0.4°C). Semicrystalline polymers have more or less perfect crystallites with different lamellae thicknesses.<sup>14</sup> A broad melting range, as observed for our samples, reflects this nonuniform structure. The maxima in the crystallization curves of PET varied between 204 and 214°C (standard deviation smaller than 1.2°C). For the backsheets B3 and B4 a double peak of PET in the crystallization curves can be seen (see Figure 3), which can be attributed to the two PET layers (core and outer layer) which vary in composition. The outer PET layer is claimed to be hydrolysis and UV resistant, thus, a different additive formulation, molecular mass distribution, and/or crystallinity of the material is expected.

Heat/crystallization enthalpies are not as precise as melting/cooling temperatures. Usually backsheets are multilayer films consisting of different polymers. As the whole weight of the sample (with all layers) is used for the calculation of the enthalpies this results in a larger uncertainty. Furthermore, small differences in the thicknesses of the individual layers within the multilayer composite of a backsheet are observed. Also the difficult sample preparation of the backsheets that have been laminated within the modules introduces additional uncertainty as a clear separation of the backsheet from the encapsulant is a very demanding task.

**Artificially Aged Backsheets (DH Storage).** The maxima of the melting peaks of the PET materials lie between 258 and 259°C with a standard deviation smaller than 0.3°C. In comparison to the initial state samples, this means a small increase in the

melting temperature of about 1 to 2°C. The melting enthalpies, on the other hand show a significant increase (see Table IV). Both facts indicate a postcrystallization, which generally appears due to aging of PET at elevated temperatures.<sup>14</sup> The mechanism is enhanced due to the storage over the glass transition temperature (~80°C) of PET.

The most significant changes of the unaged to the aged sheets can be seen in the cooling curve of the DSC runs. Changes in the DSC cooling curve are related to chemical changes in the polymers.<sup>14</sup> For example, polyolefins build a double crystallization peak when molecule chain scission happens due to aging.<sup>14,17</sup> Polycondensation polymers are susceptible to hydrolysis, which in case of PET is the cleavage of the ester groups in the polymer chain by addition of water. Hence this reaction leads to chain scission and therefore reduction of the average molecular weight. Crystalline parts of the polymer can be seen as impermeable to water vapor, therefore hydrolysis occurs solely in amorphous parts of the polymer or imperfections in the crystalline zones.<sup>18,19</sup> All produced terminal groups during artificial aging act as nucleating agents for new crystals which results in the formation of smaller crystallites and significantly higher crystallization temperatures.<sup>14,15,20</sup> Besides the higher crystallization temperature for the degraded polymer also a narrowing of the crystallization peak can be observed.<sup>20</sup> The polymer itself is more mobile and therefore the crystallization process is faster.<sup>20</sup>

The maxima of the PET crystallization peaks of the various backsheet materials were found between 217 and 222°C with a standard deviation smaller than 0.4°C. In comparison to the initial samples, this means an increase in the crystallization temperature of about 5 to 13°C. The increase in the maximum of crystallization temperature for B1, B2, and B4 are identical for

**Table IV.** PET Melting Enthalpies of Initial and Aged Single and Module Laminated Backsheets

Abbr.	Melting enthalpy (0 h)		Melting enthalpy (2000 h)	
	Sheet	Module	Sheet	Module
	[J/g]			
B1	30.9 ± 0.2	33 ± 0.7	34.8 ± 0.7	41.4 ± 2.6
B2	32.4 ± 0.4	33 ± 0.3	36.4 ± 0.9	41 ± 1
B3	25.6 ± 0.8	26.6 ± 1.4	28.2 ± 0	24.7 ± 0.2
B4	29.6 ± 0.2	28.3 ± 0.2	33.7 ± 0.2	31 ± 1.4

**Table V.** Increase in the Maximum of PET Crystallization Temperatures for the Initial to the 2000 h DH Aged Samples

	Increase in the crystallization temperature (Δ°C)	
	Sheet sample	Module sample
B1	13	13
B2	11	12
B3	8	5
B4	9	10

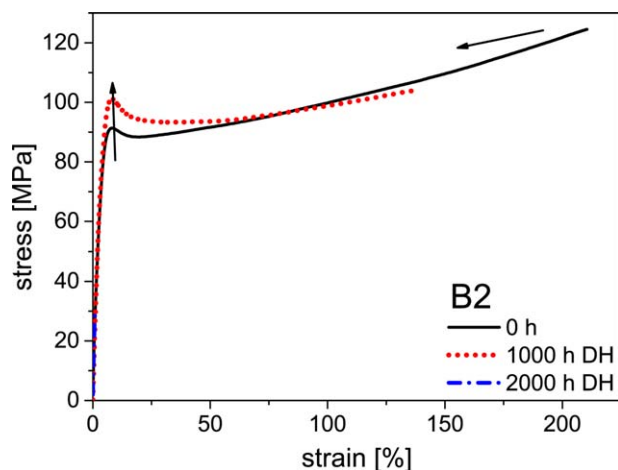


**Figure 4.** Stress–strain curves of backsheet B2 in the initial state, after 1000 h, and after 2000 h DH storage. [Color figure can be viewed in the online issue, which is available at [wileyonlinelibrary.com](http://wileyonlinelibrary.com).]

samples taken from the single backsheets and taken from the modules (see Table V). The slight temperature increase of  $+1^{\circ}\text{C}$  for the samples of the modules with B2 and B4 seems negligible to us.

In contrast to the other samples, for B3 a significant increase of the crystallization temperatures of the PET core layer was observed for the samples taken from the single sheets to those taken from the module (see Table V). The reason for this effect is maybe the additional aluminum barrier layer which is the only difference between B3 and B4. In the module, with the impermeable glass front sheet on the one side and the impermeable aluminum layer between the outer and core layer on the other side the ingress of water vapor to the PET core layer is reduced and therefore hydrolysis/degradation is reduced.<sup>21</sup> As the same shift in the crystallization temperature of the outer PET layer is measured for both sheets, single and module laminated, this assumption is supported as the pathway for water vapor from the outer side is feasible in both cases (sheet and module aging).

The DSC results showed that for reliability testing of backsheets for PV modules no significant differences between single and module aged sheets can be found. The only exception is backsheet B3 containing a gas tight Al barrier layer.

As described above evidence for the reliability and long-time stability of backsheets with PET layers can be deduced from the aging related changes as derived from the thermal analysis. DSC results of the aged backsheets taken from single and module sheets indicated postcrystallization and hydrolysis/degradation of PET. Both aging mechanisms cause embrittlement. As hydrolysis induces chain scission it gives additional possible pathways for water vapor and oxygen. Especially permeation of water vapor is often discussed in literature as a problem which can cause corrosion of metallic components as well as polymer degradation of the encapsulant.<sup>22–24</sup> To correlate the detected results with the mechanical behavior of the backsheets tensile tests were performed and the results are shown and discussed in the next section.

### Tensile Test Results

Exemplarily the stress–strain curves of backsheet B2 in the initial state and after 1000 to 2000 h aging under DH conditions are shown in Figure 4. In the initial state, the investigated materials exhibit a ductile behavior with distinct yield points. After 1000 h DH aging, an increase of the yield stress and a decrease of the strain at break value were detected for all materials. The increase of the yield stress is an indicator for physical aging like e.g. postcrystallization.<sup>8</sup> A decrease in the strain at break values can be related to chemical aging with chain scission and, therefore, with polymer degradation via hydrolysis.<sup>8</sup> The strain at break values for all materials decreased with increasing aging time (see Figure 5).

The 2000 h aged tensile test samples did not show a yield point due to the high embrittlement of the PET layers. Strain at break decreased to values below 1% (Figure 5). Breakage of samples during tensile tests starts on a defect. This defect has a notching effect with a stress concentration where crack formation begins and results in a full break of the according polymer layer. Defects can be generated mechanically from sample preparation, different thickness distributions, enclosures, bubbles, density differences occurring due to hydrolytic degradation, etc. The initiation of crack formation differs especially for aged samples as the spreading of defects is statistical. Therefore the high standard deviation of strain at break for the 2000 h DH aged samples can be attributed to differences in the crack initiation. For B3 and B4 the inner EVA layer showed a ductile behavior with a very high elongation at break after the breakage of the other (relevant) layers (see Figure 6).

The increase in the yield stress followed by the disappearance of the yield point indicated postcrystallization and the decrease in strain at break values indicated chain scission (hydrolysis). Therefore tensile tests proved to be a good tool for detecting aging in PET based backsheets. Postcrystallization and hydrolysis have also been detected via the DSC measurements and are in good correlation with the tensile test results.

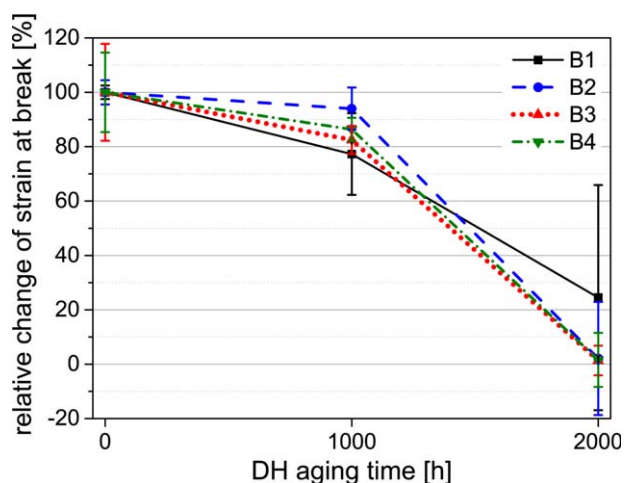


**Figure 5.** Relative change of the strain at break values of the backsheets B1–B4 in the initial state, after 1000 h and after 2000 h DH storage. [Color figure can be viewed in the online issue, which is available at [wileyonlinelibrary.com](http://wileyonlinelibrary.com).]

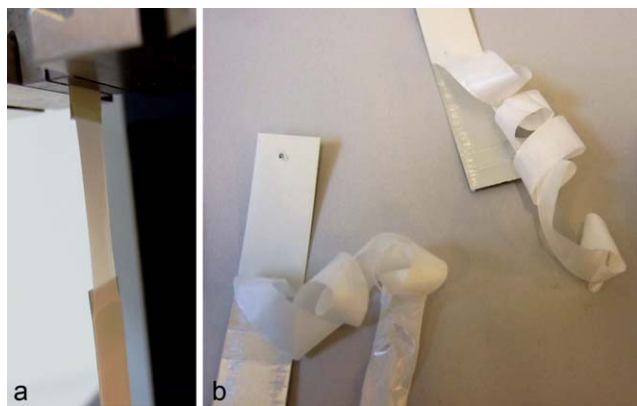


**Figure 6.** Tensile test sample of 2000 h DH aged B3 a) during and b) after testing. [Color figure can be viewed in the online issue, which is available at [wileyonlinelibrary.com](http://wileyonlinelibrary.com).]

### Oscillatory Time Sweep Test Results

Oscillatory time sweep tests, often called thermal stability tests, were performed to examine if the PET materials show time-dependent rheological properties due to thermal degradation and/or chemical reactions. Looking exemplarily on the results of backsheet B1 two characteristic phenomena are clearly visible, the strong drop of melt viscosity after DH testing and the increasing viscosity with increasing measuring time (Figure 7). The lower values of viscosity after DH storage (dashed line) result from hydrolytic degradation and by that from a decrease in molar mass. At temperatures higher than  $T_m$ , an increasing viscosity with time is a well-known effect observed in thermal stability tests of PET and can be related to (poly)condensation which is the dominating process under nitrogen atmosphere.<sup>25</sup> By that, molar mass  $M$  increases which is shown by an increasing zero shear viscosity  $\eta_0$ . This well-known relation is given by  $\eta_0 = KM^\alpha$ ,  $K$  and  $\alpha$  are polymer specific constants. Time-sweep tests were performed at  $\omega = 1 \text{ rad s}^{-1}$  and, as shown in Figure 7 (inserted graph) at this angular frequency the  $\eta_0$  is reached.

However, due to changes in the molar mass long-term rheological methods like frequency sweeps and their interpretation are

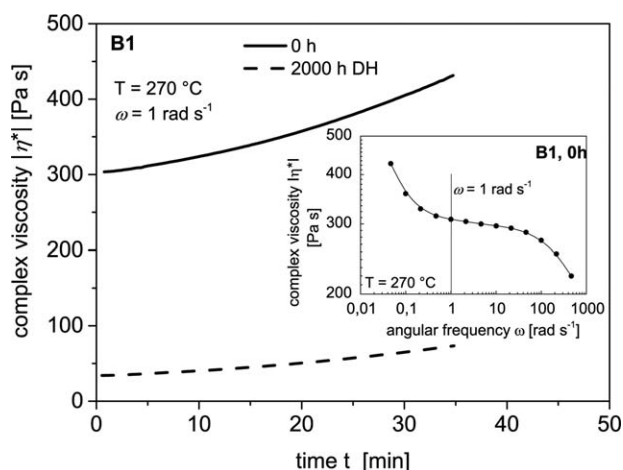


**Figure 7.** Complex viscosity  $\eta^*$  at  $\omega = 1 \text{ rad s}^{-1}$  and  $270^\circ\text{C}$  as a function of time of the core PET layer taken from an initial and aged single backsheet B1.

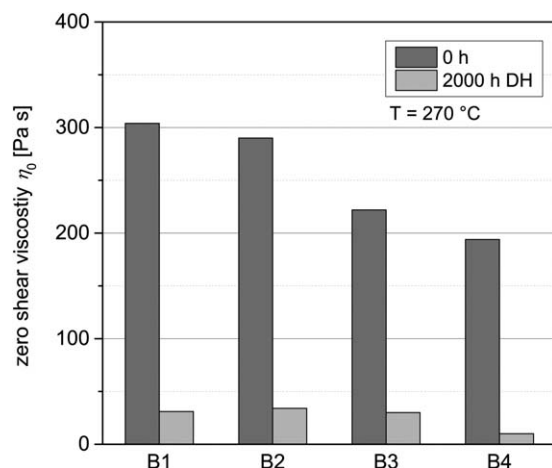


**Figure 8.** Complex viscosity  $\eta^*$  at  $\omega = 1 \text{ rad s}^{-1}$  and  $270^\circ\text{C}$  of the PET core layer taken from the initial and aged single backsheets.

an awkward procedure. Only a short time window of about 10 min (including sample load) is available.<sup>26,27</sup> Therefore, and to give a qualitative proof of chain scission (decreasing molar mass) during DH storage the  $\eta_0$  after a measuring period of 1 min was read out and compared (Figure 8). All backsheets show this strong decrease in viscosity reflecting the hydrolytic degradation.

### SUMMARY AND CONCLUSIONS

The focus of this article was the question, whether meaningful DH reliability testing of backsheets should be performed on backsheets laminated within a photovoltaic (PV) module or if testing on single backsheets reveals comparable results. Therefore four different types of backsheets were investigated, all of them containing PET core layers. Test modules using the same components (glass, encapsulant, solar cells, etc.), varying only in the backsheet used were produced and artificially aged (damp heat:  $85^\circ\text{C}/85\% \text{ RH}$  storage up to 2000 h).

The DSC results showed that for reliability testing of DH aged backsheets of PV modules no significant differences between single and module aged sheets can be found. Reliability of backsheets with PET layers can be deduced from the aging related changes in the core layer, PET. DSC curves of the aged backsheets taken from single and module sheets indicated postcrystallization (physical aging) and hydrolytic degradation (chemical aging) of PET. Both aging effects were confirmed by results from tensile testing and rheological measurements of the single unaged and aged backsheets. The most significant changes of the initial to the aged state can be derived from the cooling curve of the DSC runs. For all materials a significant increase in the crystallization temperatures were found, which can be explained by the presence of a high number of nucleation endpoints formed by chain scission of the PET molecules by hydrolytic degradation.

From the presented results it can be stated that for reliability testing of PET based backsheets under DH conditions investigations (aging characterization) on single sheets yield meaningful results which can be directly correlated to the behavior of the

backsheets laminated within a module. Exceptions are backsheets with barrier layers. This allows simplified sample preparation, lower costs and offers more testing options for the characterization of the aging induced changes of the polymeric materials.

One has to keep in mind, however, that this does NOT mean that the type of backsheet used has no influence on the aging behavior of other components within the PV modules. Measurements on the performance of the test modules before and after DH storage gave a clear indication that the permeation properties of the backsheets for water vapor and oxygen and their aging induced changes strongly influence the performance stability of the test modules.<sup>28</sup>

Further research will be done on aging of single and module laminated backsheets under humid conditions with irradiance.

This research work was performed at the Polymer Competence Center Leoben (PCCL) within the project "Analysis of PV Aging" (FFG Nr. 829918, 4. Call "Neue Energien 2020", Klima- und Energiefonds) in cooperation with the Institute of Materials Science and Testing of Plastics at the University of Leoben. The PCCL is funded by the Austrian Government and the State Governments of Styria and Upper Austria.

## REFERENCES

1. Sample, T. Failure Modes Observed in Real Use and Long-Term Exposure; PV Module Reliability Workshop: Berlin, **2011**.
2. Gambogi, W. J.; Kopchick, J. G.; Felder, T. C.; MacMaster, S. W.; Bradley, A. Z.; Hamzavy, B.; Kathmann, E. E.; Stika, T. J.; Trout, T. J.; Garreau-Iles, L. G.; Sample, T. In Proceedings of the 28th European Photovoltaic Solar Energy Conference and Exhibition; p 2846.
3. Friesen, T. PV Modules Failure Modes Observed in Real Use and Long Term Exposure; PV Module Reliability Workshop: Berlin, **2011**.
4. Stollwerck, G.; Schoeppel, W.; Graichen, A.; Jaeger, C.; Kollesch, M. In Proceedings of the 28th European Photovoltaic Solar Energy Conference and Exhibition; p 2842.
5. Reid, C.; Ferrigan, S. A.; Martinez, J. I.; Woods, J. T. In Proceedings of the 28th European Photovoltaic Solar Energy Conference and Exhibition; p 3340.
6. Oreski, G.; Wallner, G. *Solar Energy Mater. Solar Cells* **2005**, *89*, 139.
7. Oreski, G. In Proceedings of SPIE Solar Energy + Technology; SPIE: San Diego, CA, **2010**; p 77730D-1-11.
8. Oreski, G.; Wallner, G. *Solar Energy* **2005**, *79*, 612.
9. Oreski, G.; Pinter, G. In Proceedings of the 28th European Photovoltaic Solar Energy Conference and Exhibition; p 3050.
10. Hirschmann, B.; Oreski, G. In Proceedings of Centre of Excellence PoliMaT (Hg.)—The Proceedings of the Austrian/Slovenian Polymer Meeting; **2013**; p 42.
11. Oreski, G.; Wallner, G.; Lang, R. *Biosyst. Eng.* **2009**, *103*, 489.
12. International Organisation for Standardisation, Plastics – Differential Scanning Calorimetry (DSC). Part 3: Determination of Temperature and Enthalpy of Melting and Crystallization; **1999**.
13. International Organisation for Standardisation, Plastics – Determination of Tensile Properties. Part 3: Test Conditions for Films and Sheets, **1995**.
14. Ehrenstein, G. W.; Riedel, G.; Trawiel, P. Thermal Analysis of Plastics: Theory and Practice; Carl Hanser Verlag: Munich, **2004**.
15. Badia, J.; Strömberg, E.; Karlsson, S.; Ribes-Greus, A. *Polym. Degrad. Stab.* **2012**, *97*, 98.
16. Hirschl, C.; Biebl-Rydl, M.; DeBiasio, M.; Mühleisen, W.; Neumaier, L.; Scherf, W.; Oreski, G.; Eder, G.; Chernev, B.; Schwab, W.; Kraft, M. *Solar Energy Mater. Solar Cells* **2013**, *116*, 203.
17. Ehrenstein, G. W.; Pongratz, S. Beständigkeit von Kunststoffen, 1st ed.; Carl Hanser Verlag: Munich, **2007**.
18. Menges, G.; Haberstroh, E.; Michaeli, W.; Schmachtenberg, E. *Werkstoffkunde Kunststoffe*, 5th ed.; Carl Hanser Verlag: Munich, **2002**.
19. Duncan, B.; Urquhart, J.; Roberts, S. Review of Measurement and Modelling of Permeation and Diffusion in Polymers; NPL Report DEPC MPR 012; **2005**.
20. Frick, A.; Stern, C. DSC-Prüfung in der Anwendung; Carl Hanser Verlag: Munich, **2006**.
21. Koehl, M.; Heck, M.; Wiesmeier, S. *Solar Energy Mater. Solar Cells* **2012**, *99*, 282.
22. Jorgensen, G. J.; Terwilliger, K.; Barber, G. D.; Kennedy, C.; McMahon, T. J. In NCPV Program Review Meeting.
23. Barber, G. D.; Jorgensen, G. J.; Terwilliger, K.; Glick, S. H.; Pern, J.; McMahon, T. J. New Barrier Coating Materials for PV Module Backsheets: Preprint; **2002**.
24. Hülsmann, P.; Jäger, M.; Weiss, K.; Köhl, M. In SPIE 7773; Reliability of Photovoltaic Cells, Modules, Components and System.
25. Assadi, R.; Colin, X.; Verdu, J. *Polymer* **2004**, *45*, 4403.
26. Ghanbari, A.; Heuzey, M.; Carreau, P. J. *Rheol. Acta* **2013**, *52*, 59.
27. Rosu, R. F.; Shanks, R. A.; Bhattacharya, S. N. *Polymer* **1999**, *40*, 5891.
28. Voronko, Y.; Eder, G. C.; Knausz, M.; Oreski, G.; Koch, T.; Berger, K. In Progress in Photovoltaics: Research and Applications, submitted.